Atomic Spectroscopy

Article

Strontium Isotopic Fingerprinting of Atmospheric Particulate Matter by Quadrupole Inductively Coupled Plasma Mass Spectrometry

Marco Grotti,* Maria Alessia Vecchio, Dalia Gobbato, Matilde Mataloni, and Francisco Ardini

Department of Chemistry and Industrial Chemistry, University of Genoa, Via Dodecaneso 31, 16146 Genoa, Italy

Received: *November 03, 2023;* ***Revised:*** *November 29, 2023;* ***Accepted:*** *December 26, 2023;* ***Available online:*** *December 26, 2023.*

DOI: 10.46770/AS.2023.270

ABSTRACT: The strontium (Sr) isotopic composition of the atmospheric particulate samples was measured using single-quadrupole inductively coupled plasma mass spectrometry. After the multivariate optimization of the main operating conditions (sample uptake rate, spray chamber temperature, and quadrupole voltages), the $^{87}Sr/^{86}Sr$ isotopic ratio was measured with an internal precision of ~0.1% (%RSD, n=12) at the Sr concentration of 2−10 μg L^{-1} and ~0.2% at 0.5−2 μg L^{-1}. The isobaric interferences were mathematically fixed, whereas the instrumental mass bias was efficiently corrected by a combination of internal corrections based on the measurement of the $^{88}Sr/^{86}Sr$ ratio and bracketing external calibration. Finally, an optimized Sr isolation procedure produced a low procedural blank (0.05±0.01 μg L^{-1}) and good recovery (78±7%) at a low Sr concentration (0.5−2 μg L^{-1}). The applicability of the developed method was demonstrated by the analysis of a time series of PM_{10} samples collected from the Antarctic Plateau, which are characterized by a low Sr concentration and limited sample mass. The results were in excellent agreement with those published in the literature.

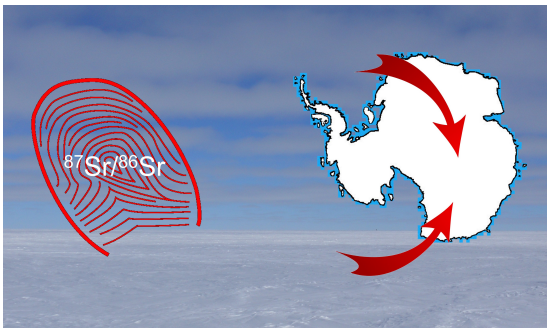

INTRODUCTION

Air pollution, especially the fine particulate matter, such as PM_{10} (airborne particulate matter with aerodynamic diameter <10 μm) and $PM_{2.5}$ (airborne particulate matter with aerodynamic diameter <2.5 μm), is a global environmental problem, a major threat to human health[1,2] and contributes to climate change.[3,4] To protect human health and the environment, pollution levels should be reduced by limiting the emissions at the source; this requires reliable source apportionment techniques.[5]

Among the methods used to trace PM sources, the use of nontraditional stable isotopic signatures (*e.g.*, Si, Fe, Cu, Zn, Pb, Hg, Sr, and Nd) has attracted increasing interest, because of the conservative behaviour and high selectivity demonstrated by these species.[6] Sr is composed of four naturally stable isotopes: ^{84}Sr (0.56%), ^{86}Sr (9.86%), ^{87}Sr (7.02%), and ^{88}Sr (82.56%). ^{87}Sr originates from the beta decay of ^{87}Rb ($t_{1/2} = 4.96\times10^{10}$ years),[7] leading to relatively large natural variations in the $^{87}Sr/^{86}Sr$ isotope ratio. Therefore, Sr isotopic signatures have been widely used to identify the origins of PM, predominantly to assess the possible natural sources of mineral dust.[8-12] Sr isotopic fingerprinting has also been proposed as a tool to identify anthropogenic PM, which originates from sources such as coal burning, waste incineration and cement plants.[13-16] Moreover, the anthropogenic Sr signature is different from the natural one, likely due to isotope fractionation during combustion processes, thus allowing the estimation of the relative contributions of natural and anthropogenic sources of PM.[17]

However, obtaining accurate Sr isotopic data is a difficult task, requiring expensive instrumentation and rigorous sample preparation procedures to achieve the best precision and avoid any bias. In particular, the Sr isotope analysis of PM has always been conducted using thermal ionization mass spectrometry (TIMS) or multi-collector inductively coupled plasma mass spectrometry (MC-ICPMS), preceded by Sr-spec resin-based chromatography

to isolate Sr from the matrix, which predominantly consists of Rb.[6] In a single study,[12] inductively coupled plasma tandem mass spectrometry was applied to the Sr isotopic analysis of PM_{10} samples using a high-efficiency microsample introduction system and reaction/collision cell technology to resolve the spectral overlap of ^{87}Rb on ^{87}Sr. In contrast, to the best of our knowledge, the use of single-quadrupole ICP-MS for the Sr isotopic fingerprinting of PM has never been reported, although it would be beneficial in terms of cost, ease of use, instrumentation availability, and sample throughput.

In this study, a method for the determination of the $^{87}Sr/^{86}Sr$ isotope ratio using single-quadrupole ICP-MS was optimized and characterized in terms of precision, uncertainty estimation, and minimum detectable concentration. The Sr separation procedure was improved to achieve satisfactory recovery at low analytical concentrations and negligible blank values. The applicability of the developed method was demonstrated by analyzing a time series of PM_{10} samples from Antarctica, which were characterized by a low Sr amount (2−6 ng).

EXPERIMENTAL

A PerkinElmer (Waltham, MA, USA) NexION 2000 ICP-MS instrument was used. The instrument characteristics and operating parameters are listed in Table 1. The sample introduction system consisted of a PFA-ST micronebulizer (Elemental Scientific, Omaha, NE, USA) connected to a glass cyclonic spray chamber whose temperature was controlled by a PC^{3X} Peltier heater/cooler system. The sample uptake rate (UR) and spray chamber temperature (T) were concomitantly optimized using a Doehlert design[18] (Table S1), whereas the cell rod offset (CRO), cell entrance/exit voltage (formerly the cell path voltage, CPV) and quadrupole rod offset (QRO) were optimized using a central composite design[19] (Table S2). The nebulizer gas flow rate was approximately 1.10 L min^{-1}, which was adjusted daily for maximum sensitivity, while keeping the oxide (CeO^+/Ce^+) and double-charge (Ce^{2+}/Ce^+) formation lower than 2.5%. The quadrupole ion deflector voltage and torch XY alignment were also optimized daily to maximize the sensitivity. Finally, the acquisition parameters (dwell time and number of sweeps) were optimized to achieve the best precision for measuring the $^{87}Sr/^{86}Sr$ isotope ratio within a suitable analysis time. The detector dead time was found to be 38 ns, according to a method by Nelms *et al.*[20]

Reagents and standards. Ultrapure water was supplied by a four-column Milli-Q ion-exchange system, fed by a reverse osmosis system Elix 3 (both from Millipore, Burlington, MA, USA). Ultrapure-grade Normatom® 67% nitric acid and 37% hydrochloric acid were purchased from VWR International (Radnor, PA, USA). Standard solutions for the daily-performance checks and tuning were provided by PerkinElmer. A single-element 1 mg mL^{-1} Sr standard solution was purchased from Merck (Darmstadt, Germany) and diluted to the required concentration with Milli-Q water.

Table 1. Instrument characteristics and operating parameters

Instrument	PerkinElmer NexION 2000
Sample introduction system	
Nebulizer	PFA−ST3 Type C MicroFlow
Spray chamber	Glass cyclonic with PC^{3X} Peltier heater/cooler
Spray chamber temperature	Studied: from 2 to 25 °C; optimal: 5 °C
Nebulizer gas flow rate	1.10 L min^{-1} (adjusted daily)
Sample uptake rate	Studied: 70-200 µL min^{-1}; optimal: 150 µL min^{-1}
Plasma source	Free-running ICP (nominal 34 MHz) with Lumicoil®
RF Power	1600 W
Plasma gas flow rate	15.0 L min^{-1}
Auxiliary gas flow rate	1.20 L min^{-1}
Interface	Triple-cone interface
Sampler	1.1 mm diameter Ni
Skimmer	0.9 mm diameter Ni
Hyper skimmer	1.0 mm diameter Al
Ion optics	Quadrupole Ion Deflector (QID)
QID voltage	−13.0 V (adjusted daily)
Reaction cell	Universal Cell Technology
Cell condition	vented (no gas)
Cell rod offset (CRO)	Studied: from −20 to +4 V; optimal: −8 V
Cell entrance/exit voltage	Studied: from −30 to +2 V; optimal: −14 V
Quadrupole rod offset (QRO)	Studied: from −10 to +4 V; optimal: −10 V
RPa (*)	0
RPq (*)	0.25
Detector	Dual analog/digital discrete dynode
Analog stage voltage	−1637 V
Pulse stage voltage	1100 V
Signal measurement	
Acquisition mode	Peak-hopping
Sweeps	Studied: 100−500; optimal: 500
Dwell time	Studied: 1−5 ms; optimal: 2 ms
Readings/replicate	10
Replicates	12
Isotopes	^{83}Kr, ^{85}Rb, ^{86}Sr, ^{87}Sr, ^{88}Sr

Note: (*) RPq=q/0.95; RPa=a/1.9, where a and q are Mathieu stability diagram parameters.

The Sr was isolated using a Sr-Spec resin (Triskem International, Bruz, France) and stored in an acid-cleaned polyethylene vial filled with Milli-Q water. Before use, the resin was cleaned three times each with Milli-Q water, three times with 6 M HCl, and three times with Milli-Q water.

The isotopic reference material SRM 987 from NIST (Gaithersburg, MD, USA) was used to determine the detector dead time, optimize the instrumental parameters, correct for instrumental mass bias, and evaluate the analytical recovery. The certified $^{87}Sr/^{86}Sr$ value is 0.710248 ± 0.000012.[21]

Samples and sample preparation. The method was applied to a time series of atmospheric particulate matter (PM_{10}) samples collected from the Antarctic Plateau in the context of the Italian

Table 2. Elution sequence for chromatographic Sr isolation using Sr-SPEC resin

Step	Repetition	Reagents
Wash	6	1.0 mL HCl (6 M, suprapur)
	3	1.0 mL H_2O (Milli−Q)
Conditioning	3	1.0 mL HNO_3 (7 M, suprapur)
Sample loading	1	1.5 mL
Matrix removal	4	1.0 mL HNO_3 (7 M, ultrapure)
Elution	6	1.0 mL H_2O (Milli−Q)

National Program of Research in Antarctica. Details of sample collection and digestion have been reported elsewhere.[12]

The Sr was isolated by extraction chromatography using 400 µL of the Sr-Spec resin according to the elution sequence summarized in Table 2. An aliquot of 1.5 mL of digested sample was loaded onto the column, and the matrix components were stripped from the resin using four 1.0 mL aliquots of 7 M HNO_3. Subsequently, Sr was eluted using six 1.0 mL aliquots of Milli-Q water, and the purified Sr fraction obtained was sublimated to dryness by freeze-drying. Finally, the sample was re-dissolved in 2.0 mL of 0.05% HNO_3, immediately prior to instrumental analysis.

Data processing. Data from the optimization study were processed using the open-source software R,[22] with the additional package CAT.[23]

The isobaric interferences of $^{86}Kr^+$ on $^{86}Sr^+$ and $^{87}Rb^+$ on $^{87}Sr^+$ were corrected by measuring the signals of $^{83}Kr^+$ and $^{85}Rb^+$ using the natural ratios $^{86}Kr/^{83}Kr = 1.502522$ and $^{87}Rb/^{85}Rb = 0.385617$, respectively.[24]

For the internal correction of instrumental mass fractionation (mass bias), three methods were tested based on the measurement of the $^{88}Sr/^{86}Sr$ ratio, which is assumed to be constant in nature (8.375209).[25] The first method assumes a linear relationship between the mass bias and the difference in mass between the two isotopes:

$$R_{true} = R_{measured}\ (1 + K\ \Delta M) \quad (1)$$

where K is the mass discrimination per mass unit, determined by measuring the $^{88}Sr/^{86}Sr$ ratio after correcting for the isobaric interference of $^{86}Kr^+$ on $^{86}Sr^+$. The second method was based on Russell's law:[26,27]

$$R_{true} = R_{measured} \left(\frac{M1}{M2}\right)^{\beta} \quad (2)$$

where β is the mass discrimination factor, determined by measuring the $^{88}Sr/^{86}Sr$ ratio, after correction for the isobaric interference of $^{86}Kr^+$ on $^{86}Sr^+$. Finally, because the estimation of the mass bias allows for a better correction of the isobaric interferences, which, in turn, leads to a better estimation of the mass bias, an iterative process can be applied until convergence.[28]

RESULTS AND DISCUSSION

Multivariate optimization of the operating conditions. The instrumental parameters that affect sample introduction and ion transmission efficiency were optimized using empirical modelling and an experimental design approach.[19,29] The combined effect of the sample UR and spray chamber T on the sensitivity at m/z=88 is shown in Fig. 1a (the model coefficients and their significance are reported in Table S3). The sensitivity improved linearly with increasing UR because of the increase in the amount of sample delivered to the ICP source, whereas the effect of T in the investigated range was less relevant. To achieve high sensitivity and minimize both the solvent load and sample consumption, UR = 150 µL min^{-1} and T = 5° C were selected as the optimal values.

The multivariate effects of the CRO, QRO, and CPV quadrupole voltages on the sensitivity and precision of the measurement of $^{87}Sr/^{86}Sr$ are shown in Figs 1b–e (the model coefficients and their significance are reported in Table S4). From the study of the response surfaces, the optimal conditions to maximize the analytical signal, and consequently improve the precision, were deduced: CRO = −8 V, QRO = −10 V, and CPV = −14 V. Under these conditions, the sensitivity at m/z = 88 was ~90 Mcps ppm^{-1} and the precision for the measurement of $^{87}Sr/^{86}Sr$ was ~0.1% at the Sr concentration of 5 µg L^{-1}.

Selection of the acquisition parameters. Because the precision of the isotope ratio depends on the total number of counts measured during each replicate, it can be improved by increasing the acquisition time per replicate.[30] However, the use of long measurement times also decreases sample throughput and increases sample consumption. In this application, the solution for instrumental analysis comes from the Sr isolation procedure, and its volume determines the sample dilution factor, and consequently, the final Sr concentration, which in turn affects the precision of the isotope ratio. To form a compromise between the two parameters, the precision of the $^{87}Sr/^{86}Sr$ isotopic ratio as a function of integration time was evaluated, along with the corresponding analysis time. The Sr concentration was set at 5 µg L^{-1}. The results are shown in Fig. 2. A sharp decrease in the RSD was obtained by increasing the integration time to 10 s, whereas a marginal improvement in the precision was observed hereafter. Therefore, an integration time of 10 s was selected to achieve good precision with a suitable analysis time (11 min) and limited sample consumption (1.65 mL). To maximize the peak hopping rate and, consequently, the instrumental noise compensation,[30] the integration time was obtained by setting a large number of sweeps

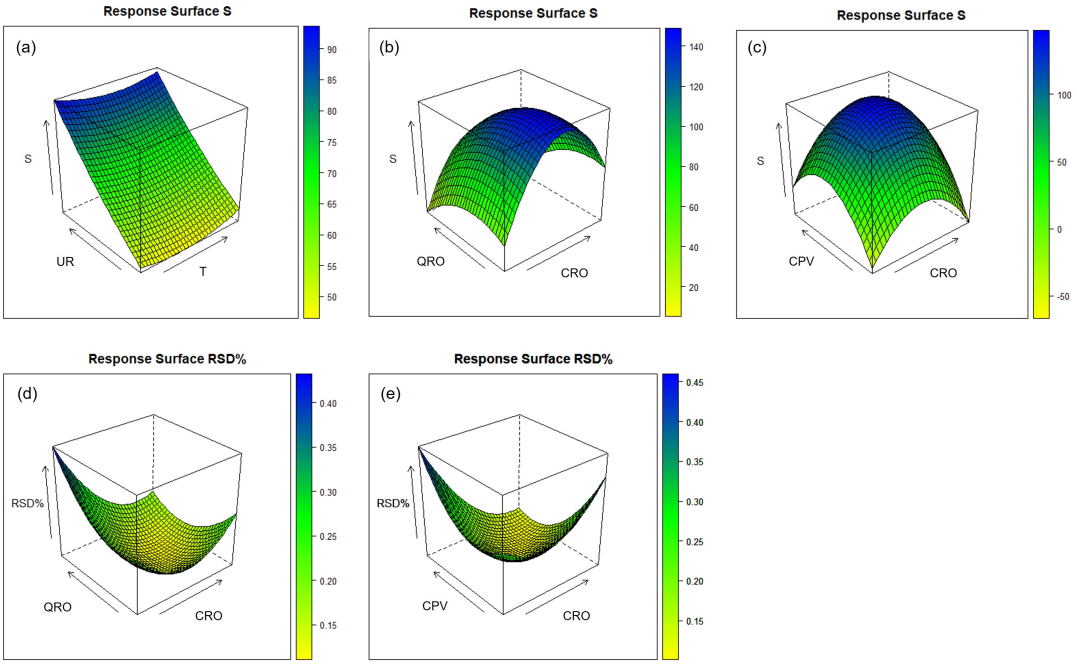

Fig. 1 Response surfaces from the multivariate study: (a) effect of sample uptake rate (UR) and spray chamber temperature (T) on sensitivity at m/z = 88; (b,c) effect of CRO, QRO and CPV on sensitivity at m/z = 88; (d,e) effect of CRO, QRO and CPV on precision of $^{87}Sr/^{86}Sr$ measurement.

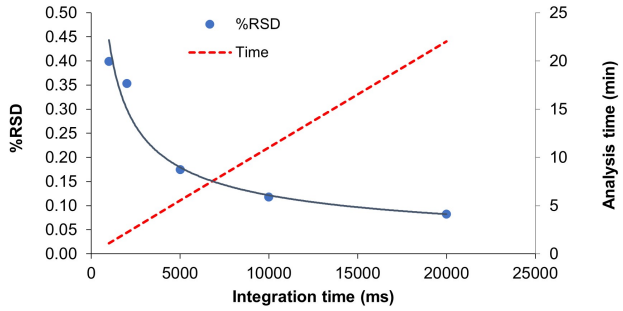

Fig. 2 Effect of the integration time on internal precision (%RSD, n=12) and analysis time (c = 5 µg L^{-1}).

Table 3. $^{87}Sr/^{86}Sr$ values in SRM 987 solutions using various mass bias correction methods (uncertainty (U) is half-width of the 95% confidence interval)

Concentration (µg L^{-1})	Linear		Russell's law		Russell's law with iterations	
	Mean	U	Mean	U	Mean	U
0.5	0.7113	0.0032	0.7113	0.0032	0.7114	0.0032
1	0.7108	0.0019	0.7107	0.0019	0.7108	0.0019
2	0.7114	0.0017	0.7114	0.0017	0.7114	0.0017
5	0.7096	0.0005	0.7096	0.0005	0.7096	0.0005
10	0.7087	0.0004	0.7087	0.0004	0.7087	0.0004
20	0.7094	0.0005	0.7094	0.0005	0.7094	0.0005

(500), along with a dwell time of 2 ms and 10 readings/replicate. For the same reason, the settling time was set at its minimum value (200 µs).

Correction for isobaric interferences and mass bias. The accuracy of isotopic ratio measurements by ICP-MS can be affected by isobaric interferences and mass discrimination effects resulting from the differences in the efficiency of ion extraction, transmission and detection as a function of analyte mass (mass bias).[30] During the measurement of Sr isotopes, potential isobaric interferences caused by Kr impurities in the Ar gas ($^{86}Kr^+$ on $^{86}Sr^+$) and remaining Rb after the Sr isolation step ($^{87}Rb^+$ on $^{87}Sr^+$) were mathematically corrected by measuring the signals of $^{83}Kr^+$ and $^{85}Rb^+$, which are free from spectral overlap.

To correct the mass bias, three models for internal correction using a constant $^{88}Sr/^{86}Sr$ ratio were tested: linear function, Russell's law, and Russell's law with iterations (further details provided in the Experimental section). The $^{87}Sr/^{86}Sr$ values obtained using these methods for the analysis of SRM 987 solutions with different Sr concentrations are compared in Table 3. It is evident that the actual differences are well below the instrumental precision; therefore, the simplest linear correction can be applied properly. The maximum departure from the certified value was 0.0015 (~0.2%), which was further corrected by an additional bracketing external calibration performed during the analysis of the PM_{10} samples.

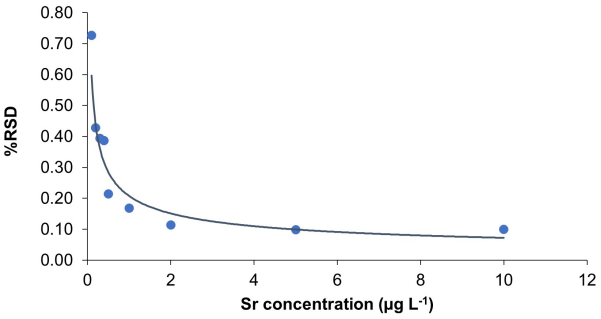

Fig. 3 Internal precision for the measurement of $^{87}Sr/^{86}Sr$ in SRM 987 solutions as a function of Sr concentration.

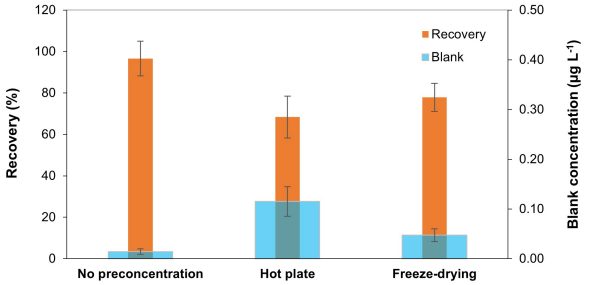

Fig. 4 Analytical recovery and procedural blank for the Sr isolation procedure.

Analytical figures of merit and uncertainty estimation. The internal precision of the $^{87}Sr/^{86}Sr$ ratio measurements with increasing Sr concentration is shown in Fig. 3. A threshold of 0.2% was selected as the lowest useful precision, and a concentration limit of 0.5 µg L^{-1} of Sr in the analytical solution was fixed. For concentrations above this limit, the impact of the instrumental and procedural blanks (0.001 µg L^{-1} and 0.05 µg L^{-1}, respectively) can be regarded as negligible. The external instrumental precision was assessed by replicated measurements of the SRM 987 solution used as bracketing standards during the analysis of PM_{10} samples, leading to a relative standard deviation of 0.08% (n = 12; c = 2 µg L^{-1}).

The uncertainty sources and their contributions to the total uncertainty were assessed according to the guide to the expression of uncertainty in measurement (GUM).[31] Through the measurement of the $^{87}Sr/^{86}Sr$ ratio isotopic ratios, the uncertainty sources were related to the dead time measurement, internal and external mass bias correction, and the mathematical correction for the isobaric interferences. In particular, the dead-time-dependent uncertainty is a function of the internal precision (which is in turn affected by the internal correction of the mass bias), the standard deviation of the dead time, and the standard deviation of the ^{86}Sr signal intensity. The uncertainty associated with the external mass bias correction is related to the internal precision of the isotope ratio measurements of the bracketing standards and the sample and to the uncertainty of the certified ratios. The total extended uncertainty was obtained by computing the square root sum of the squares of every contribution and multiplying it by the coverage factor k=2. The uncertainty was calculated from the data obtained from the analyses of the PM_{10} sample DC 10−18 (Sr concentration of 2.5 µg L^{-1}) and two bracketing SRM 987 standards (Sr concentration of 2 µg L^{-1}). The computed combined uncertainty was 0.0012, which is in good agreement with the dispersion of $^{87}Sr/^{86}Sr$ data in that sample (0.0011). The internal precision was by far the most important contributor, accounting for more than 99% of the total uncertainty, whereas the remaining contributions were negligible.

Optimization of the Sr isolation procedure. To avoid spectral overlap of the signals from the isobaric nuclides ^{87}Sr and ^{87}Rb, the analyte was isolated from the matrix by extraction chromatography using a Sr-specific resin with a crown ether as the active component.[32,33] The procedure was based on the work by De Muynck *et al.*,[34] but optimized to perform adequately at a few nanograms of Sr, such as those expected in the digests of PM_{10} samples from polar areas.

The results are shown in Fig. 4. Preliminary experiments established that high recovery (>90%; c=1−2 µg L^{-1}) can be obtained both using either 400 µL or 800 µL of resin, as well as a nitric acid concentration in the sample of 7 M or 2.8 M, the latter being the actual concentration resulting from the sample digestion procedure. Therefore, the amount of resin was set at 400 µL and the sample acidity at 2.8 M. Then, two procedures to preconcentrate the 6 mL eluates (Table 2) were compared: solvent removal by heating on a hot plate (110 °C; 24 h) and freeze-drying, both followed by sample re-dissolution with 2 mL of 0.05% nitric acid solution. In the first case, an acceptable recovery was obtained (68±10%, n= 8; c=0.5−2 µg L^{-1}); however, the procedural blank was unexpectedly high (0.12±0.03 µg L^{-1}, corresponding to 0.24±0.06 ng of Sr, n=4). In contrast, after several repetitions of the freeze-drying procedure, good recovery (78±7%, n=45; c=0.5-2 µg L^{-1}) and a low procedural blank result (0.05±0.01 µg L^{-1}, corresponding to 0.10±0.02 ng of Sr, n=8) were obtained. In particular, the analytical recovery at the Sr concentrations of 0.5, 1, and 2 µg L^{-1} was 74±7% (n=14), 79±7% (n=14), and 78±5% (n=17), respectively, in accordance with literature data.[35,36]

Application to PM_{10} samples from Antarctica. The developed method was applied to the Sr isotopic analysis of a time series of PM_{10} samples collected from the Antarctic Plateau in the context of the Italian National Program for Research in Antarctica. The Antarctic atmospheric dust is characterized by a wide range of Sr isotopic ratios (~0.713 to ~0.77).[8] Therefore, the precision achieved by this method is fully adequate to distinguish PM from the different regions. The solutions analyzed had an estimated Sr concentration of 1−3 µg L^{-1}, corresponding to an absolute amount of 2−6 ng. The obtained values (Table 4) are in good agreement

Table 4. $^{87}Sr/^{86}Sr$ isotope ratios in PM_{10} samples collected at Dome C (Antarctic Plateau) during 2018: comparison between values obtained in this study and a previous one by inductively coupled plasma tandem mass spectrometry (ICP-MS/MS) [12] (uncertainty (U) is half-width of the 95% confidence interval)

Sample	This work	U	ICP-MS/MS	U	Difference	Δ‰
DC 1-18	0.7092	0.0006	0.7066	0.0011	0.0026	3.7
DC 2-18	0.7079	0.0003	0.7083	0.0005	−0.0004	−0.6
DC 3-18	0.7085	0.0004	0.7102	0.0009	−0.0016	−2.3
DC 4-18	0.7085	0.0005	0.7049	0.0012	0.0036	5.1
DC 5-18	0.7086	0.0009	0.7076	0.0013	0.0010	1.4
DC 6-18	0.7105	0.0004	0.7080	0.0011	0.0025	3.5
DC 7-18A	0.7081	0.0006	0.7074	0.0007	0.0007	1.0
DC 7-18B	0.7088	0.0006	0.7078	0.0019	0.0010	1.4
DC 8-18	0.7093	0.0003	0.7076	0.0012	0.0017	2.4
DC 9-18	0.7090	0.0006	0.7092	0.0007	−0.0002	−0.3
DC 10-18	0.7093	0.0008	0.7089	0.0018	0.0004	0.5
DC 11-18	0.7087	0.0010	0.7064	0.0015	0.0024	3.3
DC 12-18	0.7088	0.0005	0.7067	0.0008	0.0021	3.0

with previously reported data,[12] with a better precision and a difference of 0.17±0.21%, which is within the uncertainties of the applied techniques. The precision of the isotopic data for the PM_{10} samples agrees with the uncertainty estimation discussed above. Finally, the obtained $^{87}Sr/^{86}Sr$ data (0.7089 ± 0.0004, mean and 95% confidence interval, n=13) are consistent with the isotopic signature recorded at the ice core (0.7088 ± 0.0002, n=9)[37] and snow samples (0.7094 ± 0.0002, n=130) from the same site.

CONCLUSION

Sr isotopic fingerprinting of atmospheric particulate matter using single-quadrupole ICP-MS, instead of MC-ICP-MS or TIMS, is possible and beneficial in terms of cost, ease of use, instrument availability and sample throughput, providing adequate precision to distinguish samples from different Antarctic regions.

The improved Sr isolation procedure involves the treatment of 1.5 mL sample digests, with low procedural blanks, high Sr recovery, and limited sample dilution. The optimized instrumental method allows Sr isotopic analysis of the eluates with an internal precision of ~0.1% at the part-per-billion concentration level, requiring 11 min and consuming less than 2 mL of the solution. The isobaric interferences and instrumental mass bias can be efficiently corrected using a combination of mathematical correction, internal correction and bracketing external calibration.

The reliability of the analytical results provided by the developed method was proven by analyzing several Antarctic PM_{10} samples, obtaining $^{87}Sr/^{86}Sr$ data in good agreement with previously published values and consistent with the isotopic signature of snow and ice at the same site.

ASSOCIATED CONTENT

The supporting information (Table S1-S4) is available at www.at-spectrose.com/as/home.

AUTHOR INFORMATION

Marco Grotti graduated in 1992, received his Ph.D. in Chemistry in 1996 and he is currently Full Professor of Analytical Chemistry at the University of Genoa. His research interests comprise fundamental studies in atomic spectrometry, development of new analytical methods for elemental, isotopic and speciation analysis of environmental matrices and their application to the study of polar ecosystems. In the framework of PNRA (Italian National Program for Antarctic Research) and PRA (Italian Program for Research in the Arctic) projects, he participated on seven expeditions to Antarctica and two expeditions to the Arctic, and he is responsible of the Antarctic Environmental Specimen Bank. He is the editorial board member of *Atomic Spectroscopy*. Marco Grotti is author of about 120 articles on ISI journals (h-index: 27), 2 textbooks, and over 100 congress presentations.

Corresponding Author

* M. Grotti

Email address: Marco.Grotti@unige.it

Notes

The authors declare no competing financial interest.

ACKNOWLEDGMENTS

This study was financially supported by the Italian National Program for Research in Antarctica (projects PNRA14_00091 and PNRA16_00252) and the Italian Arctic Research Program (project PRA2021-0020 BETHA-NyÅ). The purchase of NexION 2000 was supported by FESR (project Blue-Lab Net).

REFERENCES

1. A. J. Cohen, M. Brauer, R. Burnett, H. R. Anderson, J. Frostad, K. Estep, K. Balakrishnan, B. Brunekreef, L. Dandona, R. Dandona, V. Feigin, G. Freedman, B. Hubbell, A. Jobling, H. Kan, L. Knibbs, Y. Liu, R. Martin, L. Morawska, C.A. Pope, H. Shin, K. Straif, G. Shaddick, M. Thomas, R. Van Dingenen, A. van Donkelaar, T. Vos, C. J. L. Murray, and M. H. Forouzanfar, *Lancet*, 2017, **389**, 1907–1918. https://doi.org/10.1016/S0140-6736(17)30505-6
2. J. Lelieveld, J. S. Evans, M. Fnais, D. Giannadaki, and A. Pozzer, *Nature*, 2015, **525**, 367–371. https://doi.org/10.1038/nature15371
3. J. Haywood and O. Boucher, *Rev. Geophys*., 2000, **38**, 513–543. https://doi.org/10.1029/1999RG000078
4. R. Przybylak, Air Pollution in The Climate of the Arctic. Atmospheric and Oceanographic Sciences Library, Springer Cham., 2016. https://doi.org/10.1007/978-3-319-21696-6_8
5. M. Mircea, G. Calori, G. Pirovano, and C.A. Belis, European guide on air pollution source apportionment for particulate matter with source oriented models and their combined use with receptor models, Publications Office of the European Union, Luxembourg, 2020. https://doi.org/10.2760/470628
6. P. Zuo, Y. Huang, J. Bi, W. Wang, W. Li, D. Lu, Q. Zhang, Q. Liu, and G. Jiang, *TrAC-Trends Anal. Chem.*, 2023, **158**, 116866. https://doi.org/10.1016/j.trac.2022.116866
7. I. M. Villa, P. De Bièvre, N. E. Holden and P. R. Renne, *Geochim. Cosmochim. Acta*, 2015, **164**, 382–385. https://doi.org/10.1016/j.gca.2015.05.025
8. F. E. Grousset and P. E. Biscaye, *Chem. Geol.*, 2005, **222**, 149–167. https://doi.org/10.1016/j.chemgeo.2005.05.006
9. N. Dewan, B. J. Majestic, M. E. Ketterer, J. P. Miller-Schulze, M. M. Shafer, J. J. Schauer, P. A. Solomon, M. Artamonova, B.B. Chen, S. A. Imashev, and G. R. Carmichael, *ACS Sym. Ser.*, 2015, **1201**, 79–98. https://doi.org/10.1021/bk-2015-1210.ch004
10. R. M. B. O. Duarte, J. T. V. Matos, A. S. Paula, S. P. Lopes, S. Ribeiro, J. F. Santos, C. Patinha, E. F. da Silva, R. Soares, and A. C. Duarte, *Environ. Sci. Pollut. Res.*, 2017, **24**, 11006–11016. https://doi.org/10.1007/s11356-016-7793-8
11. A. Bozlaker, J. M. Prospero, J. Price, and S. Chellam, *J. Geophys. Res-Atmos.*, 2018, **123**, 1384–1400. https://doi.org/10.1002/2017JD027505
12. S. Bertinetti, E. Bolea-Fernandez, M. Malandrino, B. Moroni, D. Cappelletti, M. Grotti, and F. Vanhaecke, *J. Anal. At. Spectrom.*, 2022, **37**, 103–113. https://doi.org/10.1039/D1JA00329A
13. R.W. Hurst and T. E. Davis, *Environ. Geol.*, 1981, **3**, 363–367. https://doi.org/10.1007/BF02473525
14. D. Widory, X. Liu, and S. Dong, *Atmos. Environ.*, 2010, **44**, 3679–3687. https://doi.org/10.1016/j.atmosenv.2010.06.036
15. S. Wang, G. Hu, Y. Yan, S. Wang, R. Yu, and J. Cui, *Atmos. Environ.*, 2019, **198**, 302–312. https://doi.org/10.1016/j.atmosenv.2018.10.056
16. M. Lahd Geagea, P. Stille, F. Gauthier-Lafaye, and M. Millet, *Environ. Sci. Technol.*, 2008, **42**, 692–698. https://doi.org/10.1021/es071704c
17. L. Zhao, G. Hu, Y. Yan, R. Yu, J. Cui, X. Wang, and Y. Yan, *Atmos. Environ.*, 2019, **201**, 201–211. https://doi.org/10.1016/j.atmosenv.2018.12.050
18. D. H Doehlert, *J. R. Stat. Soc. Ser. C-Appl. Stat.*, 1970, **19**, 231–239. https://doi.org/10.2307/2346327
19. G. E. P. Box, W. G. Hunter, and J.S. Hunter, Statistics for experimenters: an introduction to design, data analysis, and model building, J. Wiley, New York, 1978. https://lccn.loc.gov/77015087
20. S. M. Nelms, C. R. Quétel, T. Prohaska, J. Vogl, and P. D. P. Taylor, *J. Anal. At. Spectrom*., 2001, **16**, 333–338. https://doi.org/10.1039/b007913h
21. W. Zhang and Z. Hu, *Atom. Spectrosc.*, 2020, **41**, 93–102. https://doi.org/10.46770/AS.2020.03.001
22. R. Core Team, R: A language and environment for statistical computing, R Foundation for Statistical Computing, Wien, Austria, 2014. https://www.R-project.org
23. R. Leardi, C. Melzi, G. Polotti, CAT (Chemometric Agile Tool), http://gruppochemiometria.it/index.php/software
24. J. R. de Laeter, J. K. Böhlke, P. De Bièvre, H. Hidaka, H. S. Peiser, K. J. R. Rosman, and P. D. P. Taylor, *Pure Appl. Chem.*, 2003, **75**, 683–800. https://doi.org/10.1351/pac200375060683
25. R. H. Steiger and E. Jager, *Earth Planet. Sci. Lett.*, 1977, **36**, 359–362. https://doi.org/10.1016/0012-821X(77)90060-7
26. W. A. Russell, D.A. Papanastassiou, and T. A. Tombrello, *Geochim. Cosmochim. Acta*, 1978, **42**, 1075–1090. https://doi.org/10.1016/0016-7037(78)90105-9
27. C. P. Ingle, B. L. Sharp, M. S. A. Horstwood, R. R. Parrish, and D. J. Lewis, *J. Anal. At. Spectrom.*, 2003, **18**, 219–229. https://doi.org/10.1039/B211527A
28. L. Balcaen, I. D. Schrijver, L. Moens, and F. Vanhaecke, *Int. J. Mass Spectrom.*, 2005, **242**, 251–255. https://doi.org/10.1016/j.ijms.2004.10.025
29. B. Benedetti, V. Caponigro, and F. Ardini, *Crit. Rev. Anal. Chem.*, 2022, **52**, 1015–1028. https://doi.org/10.1080/10408347.2020.1848517
30. F. Vanhaecke, L. Balcaen, and D. Malinovsky, *J. Anal. At. Spectrom.*, 2009, **24**, 863–886. https://doi.org/10.1039/B903887F
31. BIPM, IEC, IFCC, ISO, IUPAC, IUPAP and OIML, Guide to expression of uncertainty in measurement, Geneva, Switzerland 1995. http://chapon.arnaud.free.fr/documents/resources/stat/GUM.pdf
32. E. P. Horwitz, M. L. Dietz, and D. E. Fisher, *Anal. Chem.*, 1991, **63**, 522–525. https://doi.org/10.1021/ac00005a027
33. M. L. Dietz and P. J. Jensen, *Talanta*, 2004, **62**, 109–113. https://doi.org/10.1016/S0039-9140(03)00422-3
34. D. De Muynck, G. Huelga-Suarez, L. Van Heghe, P. Degryse, and F. Vanhaecke, *J. Anal. At. Spectrom.*, 2009, **24**, 1498–1510. https://doi.org/10.1039/B908645E
35. B. L. A. Charlier, C. Ginibre, D. Morgan, G. M. Nowell, D. G. Pearson, J. P. Davidson, and C. J. Ottley, *Chem. Geol.*, 2006, **232**, 114–133. https://doi.org/10.1016/j.chemgeo.2006.02.015
36. A. Bazzano, K. Latruwe, M. Grotti, and F. Vanhaecke, *J. Anal. At. Spectrom.*, 2017, **32**, 1004–1008. https://doi.org/10.1039/C7JA00062F
37. B. Delmonte, I. Basile-Doelsch, J.-R. Petit, V. Maggi, M. Revel-Rolland, A. Michard, E. Jagoutz, and F. Grousset, *Earth-Sci. Rev.*, 2004, **66**, 63–87. https://doi.org/10.1016/j.earscirev.2003.10.004